CRYSTAL SIZE DISTRIBUTIONS OF ILMENITE IN BASALT CLASTS FROM LUNA 16

J. L. Valenciano[1], C. R. Neal[1], and [2]S. I. Demidova [1]Department of Civil and Environmental Engineering and Earth Sciences, University of Notre Dame, Notre Dame, IN 46556, USA, [2]Vernadsky Institute of Geochemistry and Analytical Chemistry, Kosygin Street 19, Moscow 119991, Russia (jvalenc2@nd.edu, cneal@nd.edu, demidova.si@yandex.ru)

Introduction: Luna 16 landed in the northeastern part of Mare Fecunditatis, an area that is geologically similar to the landing sites of Apollo 11 and Apollo 12 as well as one of the most degraded of the near side multi-ringed basins (**Fig. 1**) [1]. Luna 16 collected approximately 100g of regolith in a 35cm long tube from between two Copernican age craters (Langrenus & Taruntius), which comprised basalts and anorthositic-noritic fragments [1]. This was the Soviet Union's first successful sample return, as well as the first ever robotic sample return from the Moon or any planetary body [2,3]. The returned regolith sample contained high-Al basalts (>12 wt.% Al_2O_3, [3-8]), similar to those from Apollo 14, but are distinct in that they contained 4-5 wt.% TiO_2 [2,3,5,8]. They were derived from LREE-enriched parental magmas [8] from at least two distinct eruptive episodes at 3347±24 Ma and 3421±30 Ma [9].

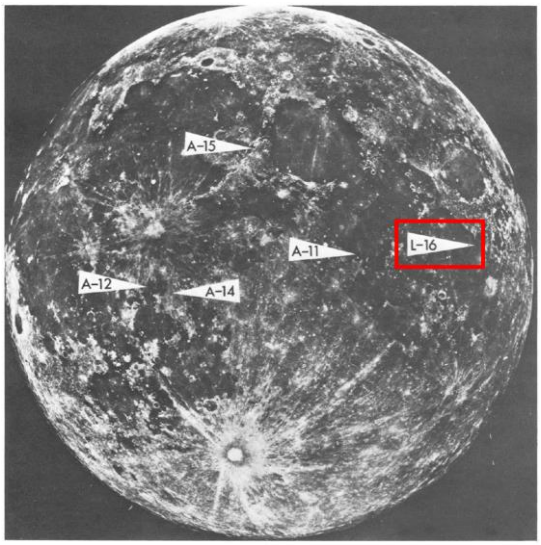

Figure 1: An image showing the landing site of Luna 16 in relation to the sites of Apollos 11-15 (modified from [1])

Samples. To conduct textural analyses, we used 4 Luna 16 basaltic fragments (gr-288, gr-289, gr-305 sample 1608 fraction >450 μm, and gr-349 sample 1611, fraction >900). Back-scattered electron (BSE) images (**Fig. 2**) and false color maps were obtained with a Tescan Mira 3 FEG SEM and accompanying Oxford Instruments EDS detector at Vernadsky Institute (Russia) with accelerating voltage of 20 kV at a working distance of 15 mm. For this paper, we determined ilmenite crystal size distributions (CSDs). CSD profiles created using the plagioclase in each of these fragments will also be presented in another abstract in this session.

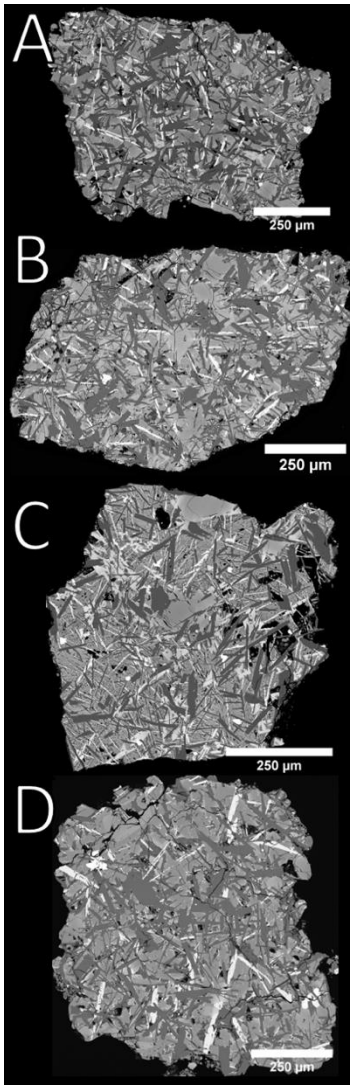

Figure 2. Backscattered-electron images of (A) gr-288, (B) gr-289, (C) gr-305, and (D) gr-349.

Methods: Crystal size distributions, a non-destructive method used to quantitatively analyze minerals in igneous samples, was implemented on the BSE images using a process similar to [10] with a few changes. *Paintshop Pro 2020* was used to trace both the sample area and individual ilmenite crystals for each of the BSE images. Between 500 – 1100 ilmenite crystals were traced for each sample using a touchscreen laptop computer and active stylus, with any crystals that overlapped or shared

boundaries traced on separate layers to avoid collecting incorrect data. Sample and crystal traces were then filled with a solid color and imported into *ImageJ*, where the known scale of each sample was used to calculate the area, best-fit ellipse, and major/minor axes. These data were then used to plot the natural log of the mineral population density versus the major axis length of each crystal (**Fig. 3**) by utilizing *CSD Corrections* [11].

Results & Discussion: Three of the samples yielded similar ilmenite CSDs (288, 289, 349), with 305 defining a steeper and shorter CSD. The slope and intercept of the CSDs are related to growth rate, residence time and nucleation rates [12,13]. Generally speaking, the steeper CSD slopes and higher intercepts = rapid cooling.

CSD profiles of these samples indicate that they all had a constant cooling rate (**Fig. 3**). Samples gr-288, gr-289, and gr-349 have nearly identical CSD profiles, presenting the possibility that they are all derived from the same basalt flow. Each of these CSDs shows a slight kink at 0.085±0.02 mm, indicating a change in conditions. Gr-305 stands out as both having the most ilmenite available to trace (~1100 crystals), a linear CSD, the smallest crystals length, which represents the fastest cooling rate. The quenched texture of the plagioclase present also sets it apart from the other samples analyzed [14].

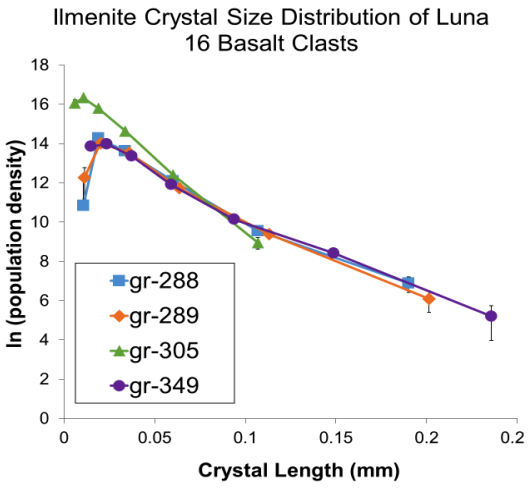

Figure 3: Ilmenite CSD profiles for gr-288, gr-289, gr-305, and gr-349. If error bars are not visible they are within the boundaries of the symbol.

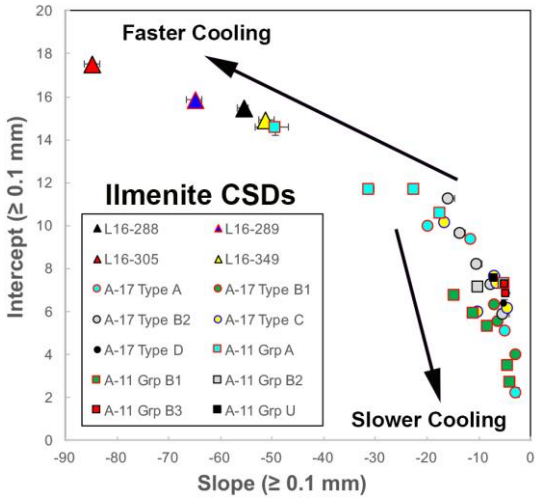

Figure 4: Slope-intercept plot for ilmenite CSDs

The Luna 16 samples exhibit steep slopes indicative of rapid, quench cooling similar to some Apollo 11 Type A basalts [15]. They also exhibit high intercepts that equate to high nucleation densities, indicating the lavas were close to ilmenite saturation upon eruption. Using the BSE images allows inclusion of smaller ilmenite crystals in the analysis and shows that the Luna 16 intermediate Ti, high-Al basalts represent the fastest cooled lunar basalts thus far analyzed for ilmenite CSDs. The basalts from Mare Fecunditatis extend the faster cooling trend on the ilmenite slope-intercept plot for lunar basalts (Fig. 4), which reveals two distinct trends that may indicate a transition from quench cooling (faster cooling trend) to textural coarsening (slower cooling trend) as hypothesized by [16].

Acknowledgements: S. I. Demidova is grateful to support of Ministry of Science and Higher Education (Russia) under the grant 075-15-2020-780 (N13.1902.21.0039)

References: [1] McCauley, J.F. & Scott, D.H. (1972) *EPSL 13*, 225-232. [2] Grieve, R.A.F. et. al. (1972) *EPSL 13*, 233-242. [3] Vinogradov A.P. (1971) *PLSC 2*, 1-16. [4] Reid J.B. et al. (1972) *EPSL 13*, 286-288. [5] Albee A.L. et al. (1972) *EPSL 13*, 353-367. [6] Keil K. et al. (1972) *EPSL 13*, 243-256. [7] Kurat G. et al. (1976) *PLSC 7*, 1301-1321. [8] Ma M.-S. et al. (1979) *GRL 6*, 909-912. [9] Cohen B.A. et al. (2001) *MaPS 36*, 1345-1366. [10] Neal, C.R. et. al. (2015) *GCA 146*, 62-80. [11] Morgan D. J., & Jerram D.A. (2006) *JVGR 154*, 1-7. [12] Marsh B.M. (1988) *Geol. Soc. Amer. Bull. 100*, 1720-1737. [13] Higgins M.D. (1996*) JVGR 70*-37-48. [14] Webb S. et al. (2021) *LPSC 52*, this meeting. [15] Xue Z. et al. (2020) *LPSC 51*, #2964. Valenciano J.L. et al. (2021) *LPSC 52*, this meeting.